# CONTROLLING OF AUTONOMOUS WIND-DE MICROGRID BY BPFF SCHEME USING FLC

**A Viswanath Reddy[1], S Sunil Naik[2]**
[1]PG Scholar, Department of Electrical Engineering, JNTU-College of Engineering, Anantapur, Andhra Pradesh, India.
[2]Lecturer, Department of Electrical Engineering, JNTU-College of Engineering, Anantapur, Andhra Pradesh, India

***Abstract:** This paper presents an active power control strategy has been developed such that when the wind alone is not able to meet the energy demand, the combination of both Wind-diesel engine supplies the load, so that the energy demand is met. Permanent Magnet Brushless DC (PMBLDC) generator is used as a wind power generator and the Incremental conductance (INC) method is used for Maximum Power Point Tracking (MPPT) along with boost converter. This output is stored into battery Storage (BS) system and surplus is supplied to the consumer loads. Squirrel Cage Induction Generator (SCIG) is used as diesel generator (DG) set. Back propagation feed forward (BPFF) control scheme is used for Voltage and Frequency (VF) control of Voltage source converter (VSC). This controller provides harmonics elimination, load leveling, and reactive power compensation and also regulates the voltage at Point of Common Coupling (PCC). The performance and the analysis of micro grid done with the help of Fuzzy Logic Controller (FLC) and Proportional Integral (PI) controller in BPFF scheme. The analysis can be done by using MATLAB/Simulink.*

***Index Terms:** Micro grid, PMBLDCG, SCIG, BPFF, MPPT, Load Leveling, Power Quality.*

## I. INTRODUCTION

In recent years the renewable energy based distributed generators (DGs) play a dominant role in electricity production, with the increase in the global warming. Conventional energy sources are limited & in declining phase now [1-2] and high cost of generation of power [3]. Distributed generation based on wind, solar energy, biomass, mini-hydro [4-6] along with use of fuel cells and micro turbines will give significant momentum in near future. Advantages like environmental friendliness, expandability and flexibility have made distributed generation, powered by various renewable and nonconventional micro sources, an attractive option for configuring modern electrical grids. In difficult geographical land where main power grid is not accessible, the concept of placing a local micro gird in combination with fossil fuel based generator sets and renewable can be materialized [7-10]. A micro grid consists of cluster of loads and distributed generators that operate as a single controllable system. A single renewable energy source may not be able to meet the load demands apart from the fact that continuous supply of energy may not be ensured (say wind is not available on a particular day in a wind farm). This makes the importance of hybrid energy systems such as wind- PV, wind-diesel along with use of battery etc. Owing to the fast controllability and response time of the diesel engines, they are quite popular for integration with wind energy conversion systems (WECS). Hence a wind diesel hybrid system is considered in this paper. In this combination, wind power is stored in BS [9-10] and excess power is utilized to supply load and if still load requirement is high and more than wind generation that deficit power is fed from the DG set [11-12]. BS design and size calculation are necessary for isolated micro grid [13-14]. Battery charging control is [15-16] for optimum charging and reliable operation of micro grid. This configuration design helps to reduce the fuel consumption and economically utilize the conventional energy resources.

In this paper, a standalone micro grid is used that constitutes Squirrel Cage Induction Generator based DG due to its low cost and low maintenance [17-19] and PMBLDC generator as Wind Energy Conversion System (WECS), the reason being its simple construction, high power density and ripple less torque [20-21]. It is connected with 3-phase rectifier, boost converter with MPPT and a battery bank for maximum power extraction an incremental conductance approach [22-23].is used to reduce the cost and to improve system reliability as it is mechanical sensor-less technique. Single voltage source converter (VSC) linked between battery bank and PCC works as Voltage and Frequency controller. Back propagation feed forward (BPFF) control scheme is used for VF control of VSC. This controller provides harmonics elimination, load leveling and reactive power compensation and also regulates the voltage at PCC. The performance and the analysis of micro grid done with the help of FLC [25] and PI controllers in BPFF scheme [24].

## II. SYSTEM CONFIGURATION AND CONTROL

Schematic diagram of Wind-Diesel micro grid is shown in the Fig.1. PMBLDC Generator used as WECS produces electrical AC power from wind energy. This energy with no ripples in the torque due to induced trapezoidal EMF and quasi square currents. This AC power converts into DC power with 3-phase diode rectifier. An inductor is attached to rectifier, makes the DC current smooth. For getting a maximum power MPPT Controller used in the boost converter. MPPT is realized with INC algorithm. BS is placed parallel with VSC and DC link. It provides stability to the micro grid during excess power generation and load leveling during low generation or peak load demand. SCIG used as DE produces AC power to the linear or nonlinear loads. It is having delta connected capacitor bank for providing reactive power externally.

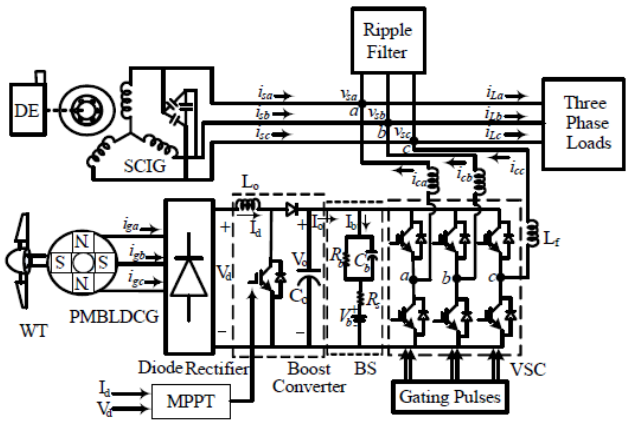


Fig.1 Schematic diagram of Wind-Diesel microgrid.

### *A. Back Propagation Feed Forward Network Controller*

BPFF is a multi layered feed forward neural network supervised learning based approach used for indirect current control of VSC. It is totally three layers. They are input layer, hidden layer and output layer. The input signal is given to the input layer first then to the hidden layer and then to the output layer. In-phase and quadrature templates of PCC voltage are obtained as, the peak terminal voltage $V_t$ is defined as,

$$V_t = \sqrt{\frac{2}{3}(v_{sa}^2 + v_{sb}^2 + v_{sc}^2)} \quad (1)$$

Where $v_{sa}$, $v_{sb}$, $v_{sc}$ are phase voltages.

The in-phase unit templates are expressed as,

$$u_{pa} = \frac{v_{sa}}{V_t} \quad u_{pb} = \frac{v_{sb}}{V_t} \quad u_{pc} = \frac{v_{sc}}{V_t} \quad (2)$$

The quadrature unit templates are defined as,

$$u_{qa} = \frac{(u_{pc} - u_{pb})}{\sqrt{3}} \quad (3)$$

$$u_{qb} = \frac{(3u_{pa} + u_{pb} - u_{pc})}{\sqrt[2]{3}} \quad (4)$$

$$u_{qc} = \frac{(-3u_{pa} + u_{pb} - u_{pc})}{\sqrt[2]{3}} \quad (5)$$

Schematic diagram of BPFF control technique is shown in the Fig. 2. it is used to generate PWM pulses for the switching of VSC by comparing the reference input currents and sensed input currents. Reference input currents are calculated with weight values of load currents. Input layer neurons in its first half portion for phase 'b' are expressed as,

$$I_{Lpb} = w + i_{La}u_{pa} + i_{Lb}u_{pb} + i_{Lc}u_{pc} \quad (6)$$

$$I_{Lqb} = w + i_{La}u_{qa} + i_{Lb}u_{qb} + i_{Lc}u_{qc} \quad (7)$$

Where w is the initial estimation of synaptic weight. Similarly phase 'a' & 'c' ($I_{Lpa}$, $I_{Lpc}$, $I_{Lqa}$ and $I_{Lqc}$) are calculated. Here for output of input layer apply the active function i.e. sigmoid function. It is expressed as,

$$X_{pb} = \frac{1}{\left(1 + e^{-I_{Lpb}}\right)} \quad (8)$$

$$X_{qb} = \frac{1}{\left(1 + e^{-I_{Lqb}}\right)} \quad (9)$$

Similarly equations for phase 'a' & 'c' ($X_{pa}$, $X_{pc}$, $X_{qa}$ and $X_{qc}$) are also calculated. The input layer outputs are given to hidden layer as inputs. They are expressed as for phase 'b',

$$I_{pbl} = w_1 + w_{pa}X_{pa} + w_{pb}X_{pb} + w_{pc}X_{pc} \quad (10)$$

$$I_{qbl} = w_1 + w_{qa}X_{qa} + w_{qb}X_{qb} + w_{qc}X_{qc} \quad (11)$$

Here $w_1$, $w_{pa}$, $w_{pb}$, $w_{pc}$ are some constants values between (0, 1) to initialize the weights. These values are updated by back propagation error correction rule. Rectified weights of phase 'b' active and reactive power components of load currents $w_{pb}$ and $w_{qb}$ at $r^{th}$ sampling time are as,

$$w_{pb}(r) = w_{pt}(r) + \eta\{w_{pt}(r) - w_{pbl}(r)\}w'_{pbl}X_{pb}(r) \quad (12)$$

$$w_{qb}(r) = w_{qt}(r) + \eta\{w_{qt}(r) - w_{qbl}(r)\}w'_{qbl}X_{qb}(r) \quad (13)$$

$w_{pa}$, $w_{pc}$, $w_{qa}$ and $w_{qc}$ are calculated in similar way. These output values are applied with active function. It is represented as,

$$w_{pbl} = \frac{1}{\left(1 + e^{-I_{pbl}}\right)} \quad (14)$$

$$w_{qbl} = \frac{1}{\left(1 + e^{-I_{qbl}}\right)} \quad (15)$$

Amplitude of the average active and reactive power components of load currents is defined as,

$$w_{pt} = \frac{a \times (w_{pal} + w_{pbl} + w_{pcl})}{3} \quad (16)$$

$$w_{qt} = \frac{a \times (w_{qal} + w_{qbl} + w_{qcl})}{3} \quad (17)$$

DC component of the weighted component is extracted through LPF. Reference active current component is computed as

$$w_{ps} = w_{pt} - w_{pw} \quad (18)$$

Where $w_{pw}$ is wind active component

$$w_{pw} = \frac{P_0}{3V_t} \quad (19)$$

The reference reactive current component is computed using a PI controller as,

$$w_{qs} = w_{qv} - w_{qt} \quad (20)$$

Where $w_{qv}(r)$ is

$$w_{qv}(r) = w_{qv}(r-1) + k_{pv}\{V_e(r)V_e(r-1)\} + k_{iv}V_e(r) \quad (21)$$

Where $V_e(r)$ is

$$V_e(r) = V_{tr}(r) - V_t(r) \quad (22)$$

The fundamental reference active and reactive power components of the input currents are computed as,

$$i^*_{spa} = w_{ps}u_{pa}, i^*_{spb} = w_{ps}u_{pb}, i^*_{spc} = w_{ps}u_{pc} \quad (23)$$

$$i^*_{sqa} = w_{qs}u_{qa}, i^*_{sqb} = w_{qs}u_{qb}, i^*_{sqc} = w_{qs}u_{qc} \quad (24)$$

$$i^*_{sa} = i^*_{spa} + i^*_{sqa}, i^*_{sb} = i^*_{spb} + i^*_{sqb}, i^*_{sc} = i^*_{spc} + i^*_{sqc} \quad (25)$$

These above reference input currents ($i^*_{sa}$, $i^*_{sb}$, $i^*_{sc}$) compared with existed input currents ($i_{sa}$, $i_{sb}$, $i_{sc}$ ) to generate PWM pulses for switching of VSC.

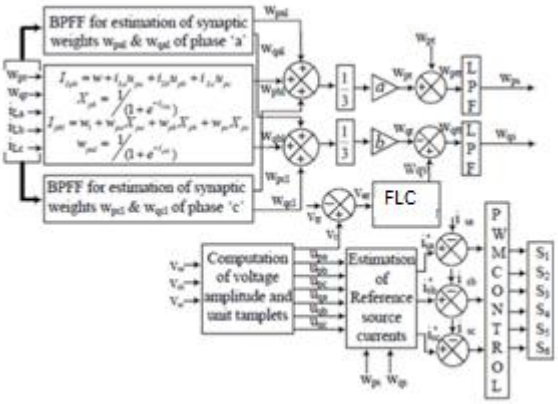


Fig. 2 Schematic diagram of BPFF control Technique.

### *B. Maximum Power Point Tracking (MPPT) Scheme*

For getting maximum power from the obtained wind power MPPT controller is used in the boost converter. For getting maximum power $dP_0/dV_0 = 0$.Where $P_0$ is output power & $V_0$ is output voltage of diode bridge. Other representation For MPPT is represented as, Z= (Id/Vd+ΔId/ΔVd) is zero. Whenever there is any change in parameter there are two cases.

- If Z becomes negative, duty cycle increases to maintain the MPPT.
- If Z becomes positive, duty cycle decreases to maintain the MPPT.

## III. FUZZY LOGIC CONTROLLER

Fuzzy Logic Controller (using the Mamdani Fuzzy Model) requires:

1. The choice of proper inputs and their fuzzification.
2. The meaning of the information and output enrollment capacities.
3. The meaning of the Fuzzy Rule Base.
4. The deffuzification of the output got after the handling of the semantic variables with the assistance of an appropriate deffuzification method.

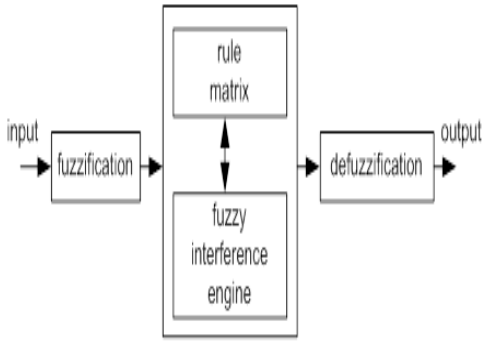


Fig. 3 Fuzzy logic strategy system

FLC controller is shown in Fig. 3 and it has Fuzzifier, Inference, Knowledge base and Defuzzifier. FLC has a five membership functions for the error, change in error and the output. The basic fuzzy sets of membership functions for the variables are as shown in the Fig. 4 to 6. The fuzzy variables are expressed by linguistic variables they are positive large (PB), positive small (PS), zero (ZE), negative small (NS), negative large (NB), for all three variables. The rules ae set based upon the knowledge of the system and the working of the system. The rule base adjusts the duty cycle for the PWM of the inverter according to the changes in the input of the FLC. The number of rules can be set as desired. The numbers of rules are 25 for the five membership functions of the error and the change in error (inputs of the FLC) shown below.

Table1: Rule for FLC

| e/Δe | ZE | NS | PS | NB | PB |
|---|---|---|---|---|---|
| ZE | ZE | PS | NS | PB | NB |
| NS | ZE | PS | ZE | PB | NS |
| PS | ZE | ZE | NS | PS | NB |
| NB | PS | PS | ZE | ZE | NS |
| B | NS | ZE | NS | PS | ZE |

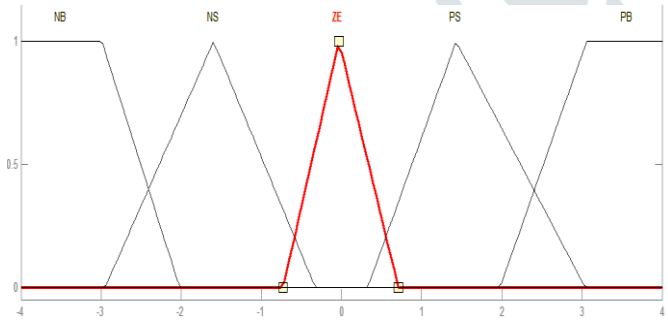


Fig. 4 Membership functions for error

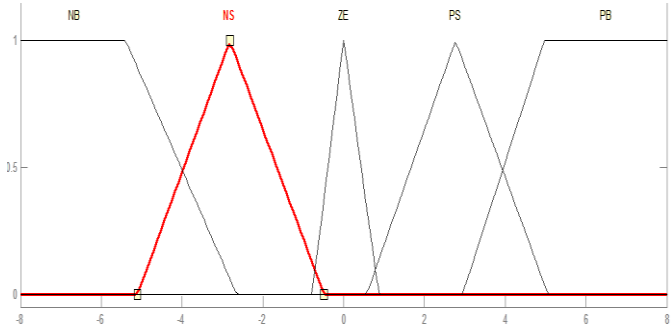


Fig. 5 Membership functions for change in error

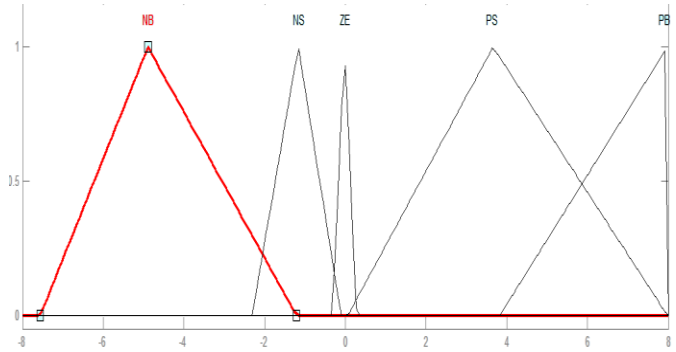


Fig. 6 Membership functions for output.

## IV. SIMULATION RESULTS

Wind-diesel micro grid model is developed in MATLAB with the ratings of 3.7 kW, 50 Hz, 230 V. simulation results are shown in following figures for effect of wind variation on non linear loads, intermediate signals and dynamic performance of microgrid during load unbalancing.

### *A. MPPT Performance and Effect of Wind Variation on Nonlinear loads*

MPPT performance with INC approach of the boost converter is shown in Fig. 7 to 9. When wind speed ($V_w$ m/s) increases from 9 m/s to 11 m/s, accordingly PMBLDCG output also increases shown in the Fig. 7 in terms of $i_{PMBLDCG.}$ This increase in power also increases the output current (Io) and output power (Po) of the boost converter shown in Fig. 9. The DC link voltage is maintained constant at 400V by the battery bank shown in Fig. 8.

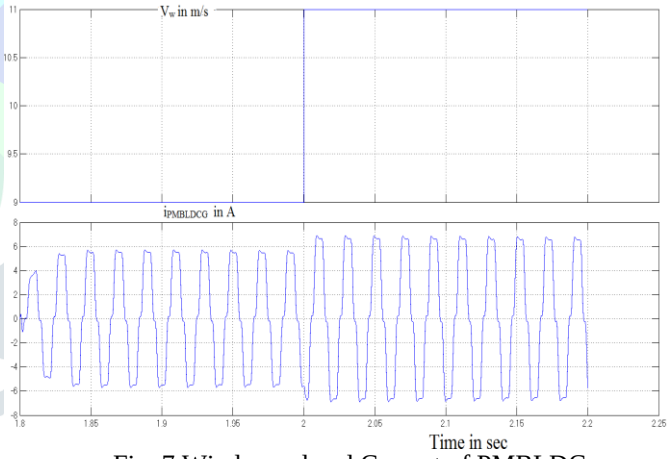


Fig. 7 Wind speed and Current of PMBLDC.

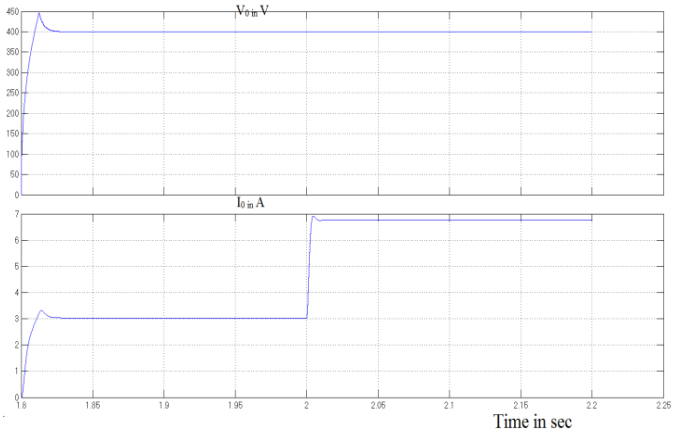


Fig. 8 Output voltage $V_0$.and Output current $I_0$ of boost converter.

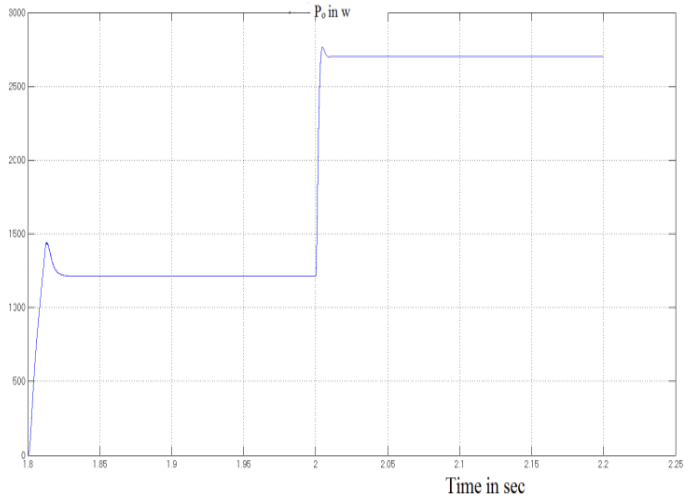


Fig. 9 Output power $P_{0.}$of boost converter.

### *B. Intermediate Signals of Microgrid at Nonlinear Loads*

For getting analysis of intermediate signals of the micro grid control under load unbalancing reference time t=3s is taken. Intermediate signals are varied according to load variation at t=3s is shown in the Fig. 10 to 12.

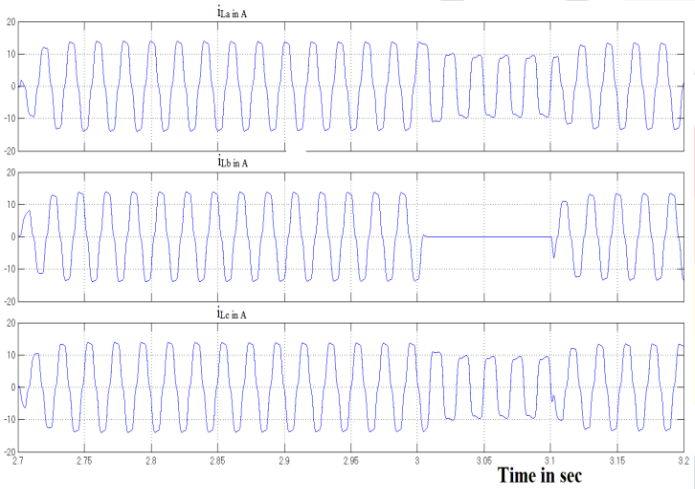


Fig. 10 Load currents variation during load unbalancing.

The intermediate signals $I_{Lpb}$ (aggregation function of input layer for active power component of load current), $I_{pbl}$ (aggregation function for active component of hidden layer), $I_{qbl}$ (aggregation function for reactive component of hidden layer), $X_{pb}$ (active component of output of input layer neuron), and $X_{qb}$ (reactive component of output of input layer neuron), Active and reactive power components of load currents ($W_{pbl}$, $W_{qbl}$), average active and reactive power components of load currents ($W_{pt}$, $W_{qt}$), weighted value of output of PI controller to regulate terminal voltage ($w_{qv}$) , active and reactive power components of reference input currents ($w_{ps}$,$w_{qs}$) are change their values according to the control requirement. With load variation ($i_{Lb}$) at t=3s, the PCC voltages ($v_{sabc}$) and source currents are maintained sinusoidal. The reference currents ($i^*_{sabc}$) are sinusoidal throughout the change.

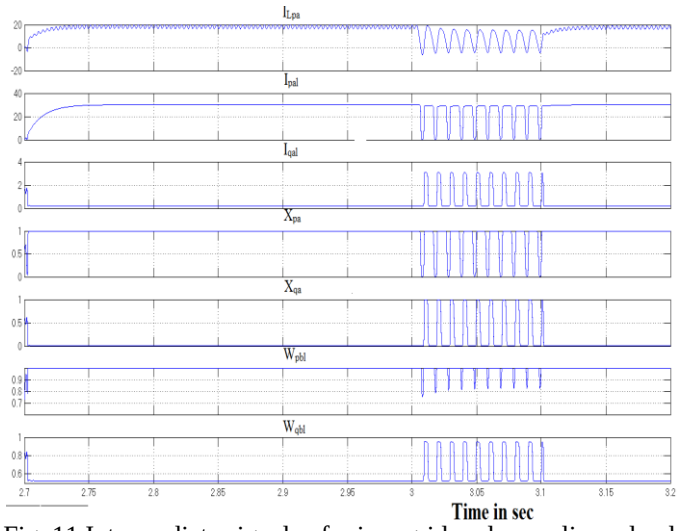


Fig. 11 Intermediate signals of micro grid under nonlinear load.

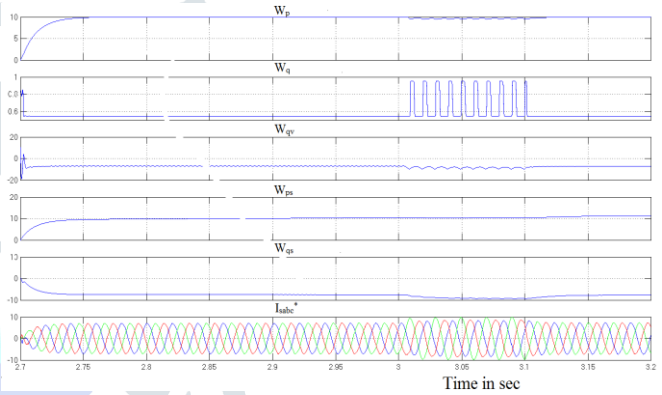


Fig. 12 Intermediate signals of micro grid under nonlinear load.

### *C. Dynamic Performance of Microgrod under Nonlinear Loads*

Dynamic conditions are analyzed by removing the load at t=3s and the balanced load is connected at t=3.1s. When $i_{Lb}$=0, other two currents $i_{La}$ and $i_{Lc}$ are in unbalanced condition shown in Fig. 13. Compensating currents ($I_{ca}$, $I_{cb}$, $I_{cc}$) are changed according to the requirement of reactive power compensation to maintain the terminal voltage (Vt) near the reference value shown in the Fig. 13. When load is low DG supplies the load as per the requirement, remaining energy is stored in BS in terms of charging current $I_{bt}$ , with constant $I_0$ from WECS shown in the Fig.14.

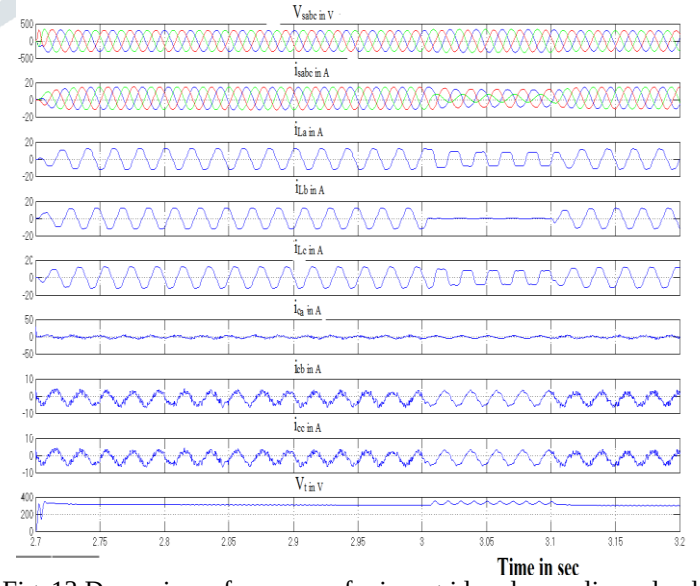


Fig. 13 Dynamic performance of micro grid under nonlinear load.

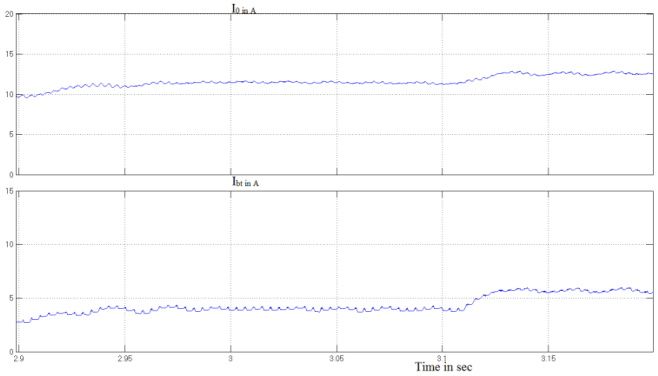


Fig. 14 Dynamic performance of micro grid under nonlinear load

Steady state analysis of algorithm in terms of line voltage $V_{sab}$, input current $i_{sb}$, and load current is shown in the Fig. 15 to 17. Results shows the performance of algorithm as the input currents and line voltages are under the distortion limit of 5% and load currents are distorted above 5%.

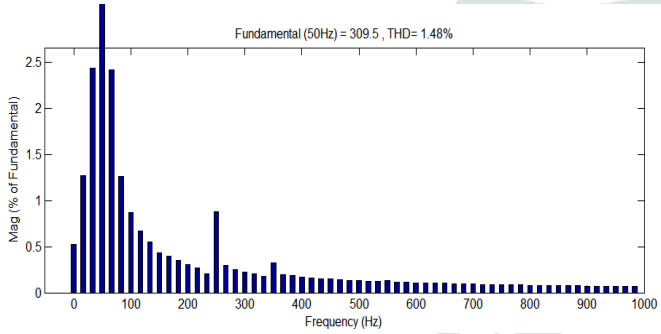


Fig. 15 FFT analysis of line voltage ($v_{sab}$)

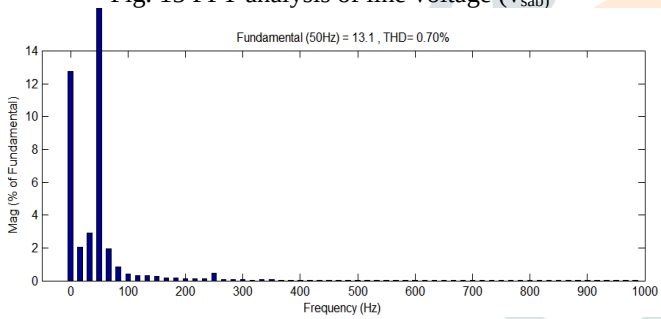


Fig. 16 FFT analysis of input current ($i_{sb}$)

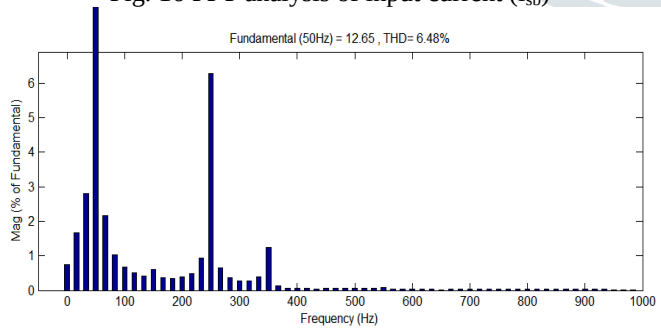


Fig. 17 FFT analysis of load current ($i_{Lb}$)

Table2: THD analysis of two controllers

| Parameters | PI | FLC |
|---|---|---|
| **Peak value of Fundamental(50Hz)** | $I_{sbpfc}$ = 15.59 | $I_{sbpfc}$ = 13.1 |
| | $V_{sbpfc}$ = 316.7 | $V_{sbpfc}$ = 309.5 |
| | $I_{lbpfc}$ =12.83 | $I_{lbpfc}$ =12.65 |
| **THD %** | $I_{sbpfc}$ =2.75 | $I_{sbpfc}$ =0.74 |
| | $V_{sbpfc}$ =3.36 | $V_{sbpfc}$ =1.48 |
| | $I_{lbpfc}$ =13.12 | $I_{lbpfc}$ =6.48 |

The above analysis shows that THD values of source current, source voltage and load voltage are improved with the FLC in BPFF when compared to the PI controller in BPFF and peak values of fundamental component are decreased.

## V. CONCLUSION

Micro grid with BPFF (using fuzzy logic controller) model is simulated in the Matlab. The main issues are harmonics reducing, load leveling, voltage regulation are improved with this model. With INC approach in MPPT controller extracted maximum power and feeds to the loads. Whenever high load and low wind occurs at a time DG and battery take care of those loads effectively with this BPFF scheme.

## REFERENCES


**[1]** M. Höök, A. Sivertsson, and K. Aleklett,"alidity of the fossil fuel production outlooks in the IPCC Emission Scenarios" Natural Resources Research, vol. 19, no. 2, pp. 63-81, June 2010.

**[2]** F. Mushtaq, W. Maqbool, R. Mat, and F.N. Ani, "Fossil fuel energy scenario in Malaysia- prospect of indigenous renewable biomass and coal resources," in proc. of IEEE Conference on Clean Energy and Technology (CEAT), 2013, 18-20 Nov. 2013, pp.232-237.

**[3]** N. Bauer, I. Mouratiadou, G. Luderer, Lavinia Baumstark, R. J. Brecha, Ottmar Edenhofer, and Elmar Kriegler, "Global fossil energy markets and climate change mitigation – an analysis with REMIND" Springer, Oct, 2013.

**[4]** Bin Wu, Y. Lang, N. Zargari, and S. Kouro, "Power Conversion and Control of Wind Energy Systems", John Wiley & Sons, Inc., Hoboken, New Jersey, 2011.

**[5]** Gilburt M. Master, "Renewable and Efficient Electric Power Systems", John Wiley & Sons, Inc., Hoboken, New Jersey, 2004.

**[6]** K.F. Krommydas, and A.T. Alexandridis, "Modular Control Design and Stability Analysis of Isolated PV-Source/Battery-Storage Distributed Gengenerationtion Systems," IEEE Journal on Emerging and Selected Topics in Circuits and Systems, vol.5, no.3, pp.372-382, Sept. 2015.

**[7]** A. Elmitwally, and M. Rashed, "Flexible Operation Strategy for an Isolated PV-Diesel Microgrid Without Energy Storage," IEEE Trans. on Energy Conversion, vol.26, no.1, pp.235-244, March 2011.

**[8]** Miao Zhixin, A. Domijan, and Fan Lingling, "Investigation of Micro grids With Both Inverter Interfaced and Direct AC-Connected Distributed Energy Resources," IEEE Transactions on Power Delivery, vol.26, no.3, pp.1634-1642, July 2011.

**[9]** M. Arriaga, C.A. Canizares, and M. Kazgenerationni, "Renewable Energy Alternatives for Remote Communities in Northern Ontario, Canada," IEEE Trans. on Sustainable Energy, vol.4, no.3, pp.661-670, July 2013.

**[10]** Dong-Jing Lee and Li Wang, "Small-Signal Stability Analysis of an Autonomous Hybrid Renewable Energy PowerGengenerationtion/Energy Storage System Part I: Time-Domain Simulations," IEEE Trans. on Energy Conversion, vol.23, no.1, pp.311-320, March 2008.

**[11]** B. Singh, R. Niwas, and S. Dube, "Load Leveling and Voltage Control of Permanent Magnet Synchronous Generator Based DG Set for Standalone Supply System,"

*IEEE Transactions on Industrial Informatics*, vol.10, no.4, pp.2034-2043, Nov. 2014.

**[12]** S. Singla, Y. Ghiassi-Farrokhfal, and S. Keshav, "Using Storage to Minimize Carbon Footprint of Diesel Generators for Unreliable Grids," *IEEE Transactions on Sustainable Energy*, vol.5, no.4, pp.1270-1277, Oct. 2014

**[13]** A. Arabali, M. Ghofrani, M. Etezadi-Amoli, M.S. Fadali, "Stochastic Performance Assessment and Sizing for a Hybrid Power System of Solar/Wind/Energy Storage," *IEEE Transactions on Sustainable Energy*, vol.5, no.2, pp.363-371, April 2014.

**[14]** B. Singh, and S. Sharma, "Design and Implementation of Four-Leg Voltage-Source-Converter-Based VFC for Autonomous Wind Energy Conversion System," *IEEE Transactions on Industrial Electronics*, vol.59, no.12, pp.4694-4703, Dec. 2012.

**[15]** Hongyu Zhu, Donglai Zhang, H.S. Athab, Bin Wu, and Yu Gu, "PV Isolated Three-Port Converter and Energy-Balancing Control Method for PV-Battery Power Supply Applications," *IEEE Transactions on Industrial Electronics*, vol.62, no.6, pp.3595-3606, June 2015 .

**[16]** M. Hosseinzadeh, and F.R. Salmasi, "Power management of an isolated hybrid AC/DC micro-grid with fuzzy control of battery banks," *IET on Renewable Power Generation*, vol.9, no.5, pp.484-493, 2015.

**[17]** B. Singh, and J. Solanki, "Load Compensation for Diesel Generator-Based Isolated Generation System Employing DSTATCOM," *IEEE Transactions on Industry Applications*, vol.47, no.1, pp.238-244, Jan.-Feb. 2011.

**[18]** R. Niwas, and B. Singh, "Solid-state control for reactive power compensation and power quality improvement of wound field synchronous generator-based diesel generator sets," *IET* on *Electric Power Applications*, vol.9, no.6, pp.397-404, 2015.

**[19]** G. Pathak, B. Singh, and B.K. Panigrahi, "Control of Wind-Diesel Microgrid using Affine Projection-Like Algorithm," *IEEE Transactions on Industrial Informatics, Early Access.*

**[20]** B.K. Bose, *"Modern Power Electronics and AC Drives"*, Prentice Hall PTR, Upper Saddle River, New Jersey, 2002.

**[21]** Bhim Singh, and Shailendra Sharma, "PMBLDC based standalone wind energy conversion system for small scale applications," *Inter. Journal of Engg. Science and Tech.*, vol. 4, no. 1, pp. 65-73, 2012.

**[22]** Snehamoy Dhar, R. Sridhar, and Geraldine Mathew, "Implementation of PV cell based standalone solar power system employing incremental conductance MPPT algorithm," in *Proc. of International Conference on Circuits, Power and Computing Technologies (ICCPCT), 2013*, pp.356-361, 20-21 March 2013.

**[23]** M.A. Elgendy, B. Zahawi, and D.J. Atkinson, "Assessment of the Incremental Conductance Maximum Power Point Tracking Algorithm," *IEEE Trans. on Sustainable Energy*, vol.4, no.1, pp.108-117, Jan. 2013.

**[24]** G. Pathak, B. Singh, and B.K. Panigrahi, "Back propagation algorithm based controller for autonomous wind-DG microgrid," in proc. of *6th IEEE Power India International Conference (PIICON)*, pp.1-5, 5-7 Dec. 2014.

**[25]** E.H. Mamdani, Application of fuzzy algorithms for control of simple dynamic plant, Proc. IEEE 121 (12) (1974) 1585–1588.